Hole–hole interaction in carbon fibre/epoxy laminates under uniaxial compression

C. SOUTIS, N.A. FLECK* and P.T. CURTIS†*

(University of Cambridge/† Royal Aerospace Establishment, UK)*

This paper describes the static compressive response of T800/924C carbon fibre/epoxy $[(\pm 45/0_2)_3]_s$ laminates containing a single or two circular holes. Penetrant-enhanced X-ray radiography, laminate deply and scanning electron microscopy are employed to observe damage initiation and propagation. Failure is due to 0° fibre microbuckling surrounded by delamination. For all geometries investigated, the microbuckled region initiates at the hole boundary at approximately 80% of the failure strength. The microbuckle band extends stably under increasing load before becoming unstable at a critical microbuckle length of 2–3 mm. The final fracture surface is almost perpendicular to the loading direction. A two-dimensional finite element analysis is used to study the interaction effect between a pair of 5 mm diameter holes as a function of hole spacing; for no interaction the hole centres should be placed at least four hole diameters apart.

Key words: *composite materials; laminates; holes; compressive strength; damage mechanisms; hole–hole interaction*

A limiting design feature of carbon fibre/epoxy laminates is their low compressive strength (60–70% of tensile strength) due to fibre instability. Although the composite structure may not buckle in compression on the macroscopic scale, the individual fibres fail by microbuckling[1,2].

Several investigators[3,4] have examined the behaviour of notched composite laminates and found that a single hole reduces the compressive strength of the laminate by more than 40%. It is therefore important to take account of this notch sensitivity when designing composite components. In addition to the effects of isolated holes, possible hole–hole interactions need to be considered. This is important for the positioning of bolt holes and for the assessment of in-service damage which may comprise a number of closely spaced defects. The hole–hole interaction problem has been addressed for tensile loading by Curtis and Dorey[5]; it does not appear to have been investigated for compression.

In this paper the results of a series of uniaxial compressive tests are presented for a T800/924C carbon/epoxy laminate containing a single and two circular holes. X-ray radiography, deply and sectioning studies are used in order to determine the compressive failure mechanisms. An elastic two-dimensional finite element analysis is performed in order to calculate the stress distribution in the region near the holes and to find the minimum hole–hole separation for no hole interaction.

EXPERIMENTAL

Material and lay-up

The material used is Toray T800 carbon fibres in a 34% volume fraction of Ciba-Geigy 924C epoxy resin. Pre-impregnated tapes of thickness 0.125 mm were laid up by hand into 1 m by 0.3 m panels of a $[(\pm 45/0_2)_3]_s$ balanced lay-up with the ±45° plies on the outside. The laminates were cured in an autoclave at the Royal Aerospace Establishment, Farnborough, at a temperature of 170°C for one hour and subsequently post-cured for four hours at 190°C. The quality and void content of the moulded laminates was checked using ultrasonic C-scanning. The test material was kept in an ambient laboratory air environment prior to use.

Specimen design considerations

In order to develop a satisfactory procedure for the design of a compressive test specimen for composite laminates, the following constraints need to be considered.

1) Compressive failure should occur at lower loads than the Euler buckling load; this requires a sufficiently short gauge length.
2) Angle-ply laminates suffer a premature grip failure when the non-axial fibres run continuously from one end of the test section to the other[6]. In order to ensure that the $\pm\theta°$ fibres run across the full width

0010-4361/91/010031-08

of the specimen, the gauge length L is chosen as

$$L = W\left(1 + \frac{1}{\tan\theta}\right)$$

where W is the specimen width and θ is the angle between the fibres and the loading axis.

) End-tabs are required in order to transfer load smoothly from the grips to the specimen.

The specimen geometry used in the current test programme was based on that recommended by CRAG test methods[7]. Specimens of dimensions 245 × 50 mm were cut from the 1 × 0.3 m panels, and reinforcement tabs of aluminium were bonded given a gauge length of 116 mm. The end-tabs were abraded and etched prior to bonding to the specimens with a Ciba-Geigy Redux 312/5 adhesive.

Circular holes of diameter d = 5 mm were drilled symmetrically about the specimen mid-point. Four different hole configurations were tested as shown in Fig. 1: (a) a single hole; (b) a pair of holes in the transverse direction; (c) two holes in the longitudinal direction; and (d) two holes at 45° to the loading axis. For the two hole configuration the hole centre–centre spacing a ranged from $a = 1.5d$ to $a = 3.5d$. The holes were machined using a tungsten carbide bit to minimize fibre damage at the hole boundary. Excessive drilling damage induces local delamination which can cause out-of-plane microbuckling and hence premature specimen failure.

In order to measure the strength of the multidirectional material, five unnotched (plain) specimens of dimensions 245 × 30 mm were tested.

Mechanical tests

The static compressive tests were performed using a screw-driven machine at a cross-head displacement rate of 0.017 mm s^{-1}.

The specimens were loaded by shear action using compressive wedge grips. An anti-buckling device was employed to prevent Euler buckling[7]. Its window size was 90 mm long by 38 mm wide (20 mm for unnotched specimens), based on the decision that local buckling

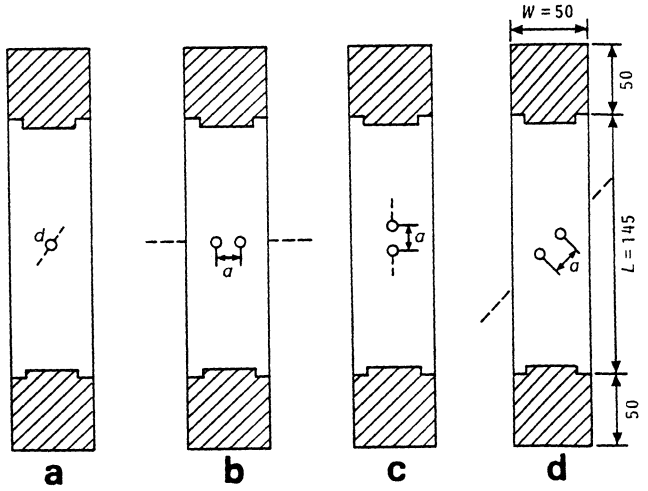

Fig. 1 Geometry of notched specimens

associated with delamination around the holes should not be restrained, but that the specimen should be restrained from general buckling. The clearance between the specimen and the buckling restraint was less than 0.3 mm. Teflon tape was used on the inside surfaces of the guide bars to reduce friction. Thus, anti-buckling guides increase the flexural stiffness of the laminate but carry no load.

Foil strain gauges were bonded to both faces of the specimens; they were used to monitor failure strains and to check that there was no significant bending.

Damage evaluation techniques

Most of the notched specimens were loaded to failure. Some were loaded almost to the failure load and then removed from the test machine. The existing damage was observed by a variety of techniques: penetrant-enhanced X-ray radiography, laminate deply and scanning electron microscopy, and sectioning and examination by light microscopy. The section studies helped to clarify damage patterns appearing on the X-ray radiographs; on an X-ray radiograph fibre microbuckling resembles a crack.

TEST RESULTS AND DISCUSSION

Unnotched specimens

The 0° unidirectional compressive properties of the T800/924C composite system were obtained from previous investigations[8,9] and are presented in Table 1 together with the compressive properties of the unnotched multidirectional $[(\pm 45/0_2)_3]_s$ material. The tensile material properties of the T800/924C system are given in Table 2 for comparison. It can be seen that the compressive strength of the unidirectional laminate is only 70% of the tensile strength.

Table 1. Compressive fracture stress σ_f, failure strain ϵ_f and Young's modulus E_{11} parallel to 0° fibres. Data is for unnotched specimens in compression

Lay-up	σ_f(MPa)	ϵ_f(%)	E_{11}(GPa)
0°	1615	1.12	161
$[(\pm 45/0_2)_3]_s$	810	1.10	85

Table 2. Measured tensile properties of T800/924C

Lay-up	Tensile strength (MPa)	Failure strain (%)	Young's modulus* (GPa)
0°	2320	1.26	168
90°	63	0.65	9.25
±45°	210	6.25	19.6

* Secant moduli at 0.25% strain
Poisson's ratio, ν_{12} = 0.34
Shear modulus, G_{12} = 6.0 GPa

The typical stress/strain compressive responses of the unidirectional and multidirectional laminates are shown in Fig. 2. The strain was measured by axial strain gauges which were placed far from the failure plane. The failure strain of the two laminates is almost equal, suggesting that the ±45° plies have little influence on the response of the 0° plies. Catastrophic failure occurs by microbuckling of the 0° fibres within the specimen's gauge length, see Fig. 3(a). The buckled fibres break at

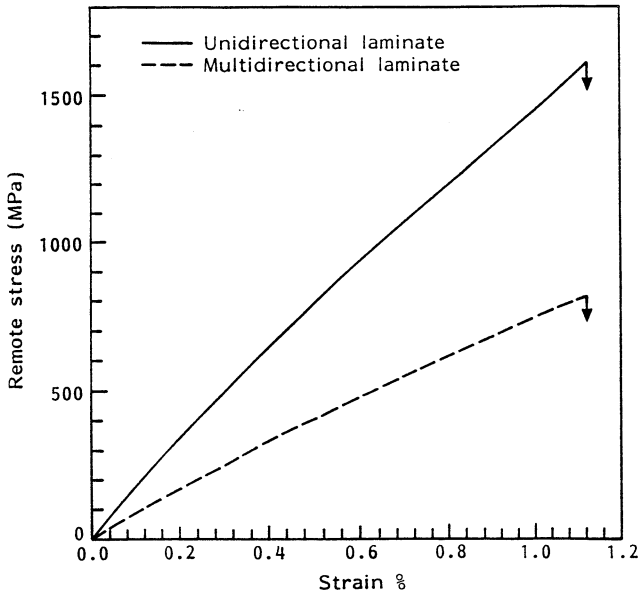

Fig. 2 Compressive stress/strain response of T800/924C unidirectional and multidirectional laminates

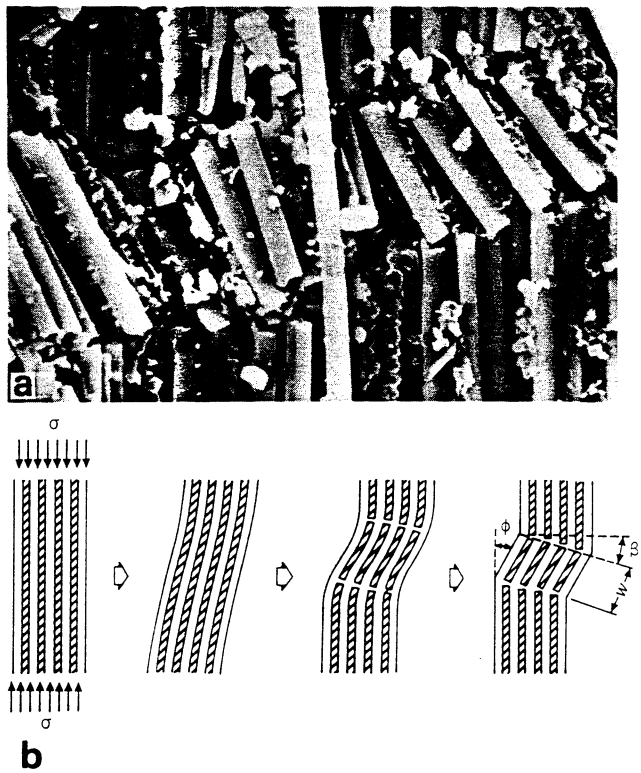

Fig. 3 (a) Fibre microbuckling mode. Two planes of fracture formed creating a kink band of length 50 μm (fibre diameter = 5.5 μm). (b) A schematic showing the geometry of the microbuckling mode: β = boundary inclination angle; φ = fibre orientation angle; w = microbuckle width

two points creating a kink band inclined at an angle β = 10–20° to the horizontal axis; they rotate by approximately 30° from the loading axis. The length of the broken segments is 8–10 fibre diameters (d_f = 5.5 μm). A schematic representation of the fibre microbuckling mode is shown in Fig. 3(b), together with the geometric parameters that define it.

In order to study the compressive failure of the unnotched laminates in greater detail it is necessary to detect the initiation of damage. In plain uniformiy stressed specimens this is difficult to achieve because failure occurs catastrophically. However, if a hole is made in the test-piece, it causes magnification of the stresses around the hole; the high local stresses result in stable microbuckling near the hole. In the following sections we describe compressive failure in notched laminates.

Specimens with a single hole

In this section a summary of the damage in the single hole laminate is presented. A thorough description is given in Reference 9.

Stress/strain data. Five specimens with a 5 mm diameter hole were tested in order to determine their failure loads. They failed from the hole in a transverse direction to the loading axis. Post-failure examination shows much delamination and fibre microbuckling along the plane of fracture but little damage away from the hole, Fig. 4(a).

The average gross section failure stress of the single hole specimens was 430 MPa compared with 810 MPa for the unnotched strength. The notched specimens exhibited less than 5% scatter in strength, indicating that the hole controls the fracture strength rather than a defect remote from the hole. A plot of the remote stress as a function of the remote axial strain for a selected specimen is shown in Fig. 4(b); strain gauge measurements in the vicinity of the hole are included in the figure. The gauges 2 and 3 (see the inset of Fig. 4(b)) show higher strains than that of the remote gauge because they are located within the strain concentration surrounding the hole. Gauge 2 is placed inside the hole, the centre-line of gauge 3 is placed 1 mm from the hole edge and the centre-line of gauge 4 is placed 3 mm from the hole edge. The ratio of measured strain ϵ_{yy} to applied strain ϵ^{∞} given by the gauge 2 inside the hole is 3.4, which is in good agreement with the finite element value of 3.48 obtained in Reference 9. Gauge 4, located 3 mm from the hole edge in the transverse direction, recorded a strain equal to the remote axial strain. At approximately 85% of the failure strength, the damage zone grows underneath gauges 2 and 3 and they detect an increase in strain concentration, see Fig. 4(b).

Damage mechanisms. The damage in the specimens with a single hole was evaluated by using penetrant-enhanced X-ray radiography[10]. The location and nature of damage in individual plies was confirmed by using the deply technique[11]. Each ply of the laminate was peeled away and was then examined in the scanning electron microscope. At low loads, no damage is evident on the faces or in the bore of the hole. As the

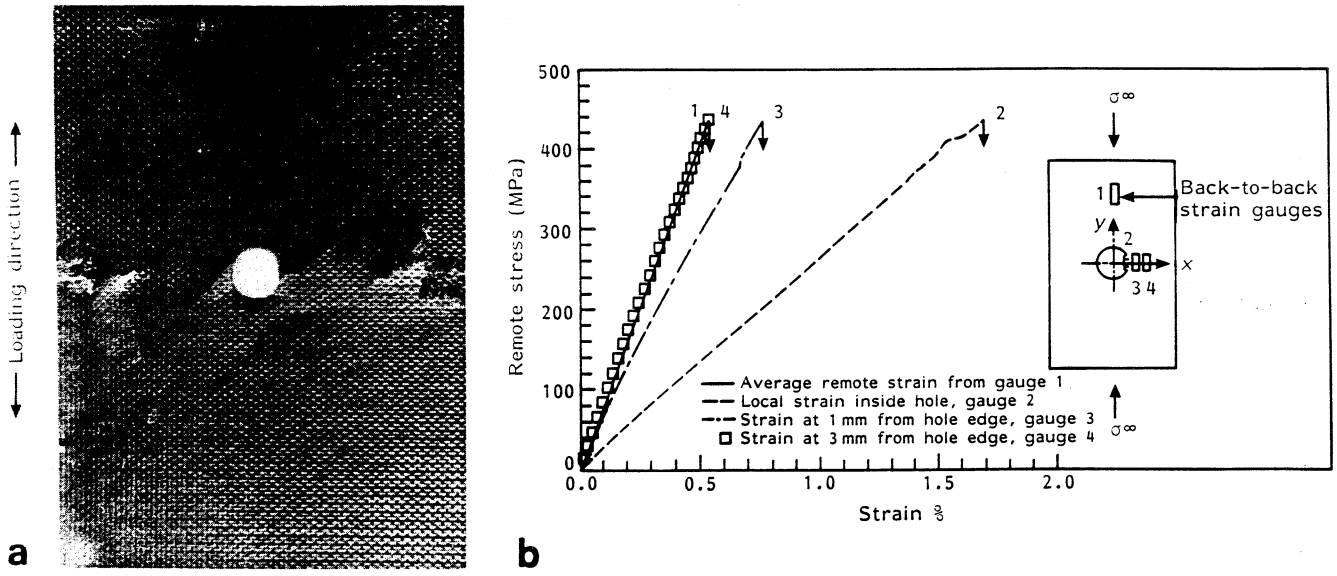

Fig. 4 (a) Overall failure of notched specimen showing local delamination, matrix cracking in the 45° plies and fibre breakage (d = 5 mm). (b) Compressive stress/strain response of specimen with one hole (d = 5 mm)

load is increased to 75% of the failure strength 0° splitting occurs at the top and bottom of the hole boundary. Fibre microbuckling surrounded by delamination develops at the edges of the hole at 80–85% of the ultimate strength and grows with increased applied load across the specimen section, see Fig. 5. In order to allow for microbuckling the 0° plies delaminate from the ±45° plies. Delaminations appear as dark shaded regions and fibre microbuckling as a series of cracks in the radiograph. When the damage zone reaches a critical length of approximately 2 mm the laminate fails catastrophically.

In the next section the damage development in specimens with two holes is described in detail.

Specimens with two holes

1. Line of holes transverse to the loading axis

Strength data. Two holes were placed symmetrically about the centre of the specimen such that the line joining hole centres is transverse to the loading axis. Five hole spacings were investigated ranging from $a = 1.5d$ to $a = 3.5d$, where a is the hole centre–centre spacing. At least five tests were performed for each hole configuration. All specimens failed through the holes; typical overall failure of the notched laminate is illustrated in Fig. 6(a). Considerable delamination and fibre breakage takes place along the line of fracture but little damage occurs away from the holes. The failure strength is 40% that of the unnotched laminate. The remote stress/strain compressive response for the a/d = 1.5 geometry is shown in Fig. 6(b). The local axial in-plane strains at the centre of the specimen and at the edge of one of the outer holes were measured using strain gauges 2 and 3, respectively. The strain measured by gauge 2 is more than three times the remote strain, see Fig. 6(b). Marked non-linearity in response is shown by gauge 2, corresponding to the development of damage between the holes at low loads.

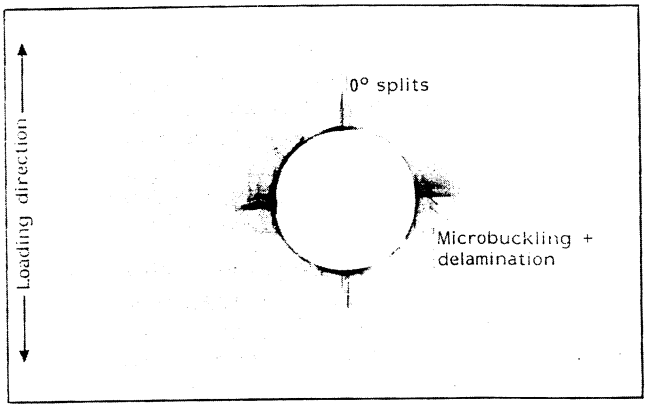

Fig. 5 X-ray radiograph taken at 85% of laminate's failure strength. Damage consists of 0° splits, few 45° matrix cracks and fibre microbuckling surrounded by delamination (d = 5 mm)

The failure load for the specimens with two holes P_{oo} is normalized by the failure load for a single hole specimen P_o, and is plotted against a/d in Fig. 7. The normalized failure load P_{oo}/P_o increases with increasing a/d as expected. If failure is governed by net sectional area we expect P_{oo}/P_o to asymptote to a value of 0.9. Instead, we find that P_{oo}/P_o asymptotes to 0.95. We define, arbitrarily, hole–hole interaction to occur when P_{oo}/P_o is less than the value 0.9 calculated on the basis of net sectional area. Thus, we deduce from Fig. 7 that hole–hole interaction ceases for $a/d > 2.5$.

If the composite material was a perfectly brittle solid, failure would occur when the maximum stress in the specimen attains a critical value. The normalized failure load P_{oo}/P_o would be coincident with the ratio of stress concentration factors at the edge of a hole in the single hole specimen K_o, and the stress concentration factors at the outer edge of a hole in the two hole specimen K_{oo}. This is not the case, see Fig. 7. For $a/d <$ 2.5 failure occurs at a lower load than predicted for a perfectly brittle, notch-sensitive solid. This is rationalized by the observation that sub-critical damage in the form of microbuckling and delamination occurs in both the specimen containing a single hole and the speci-

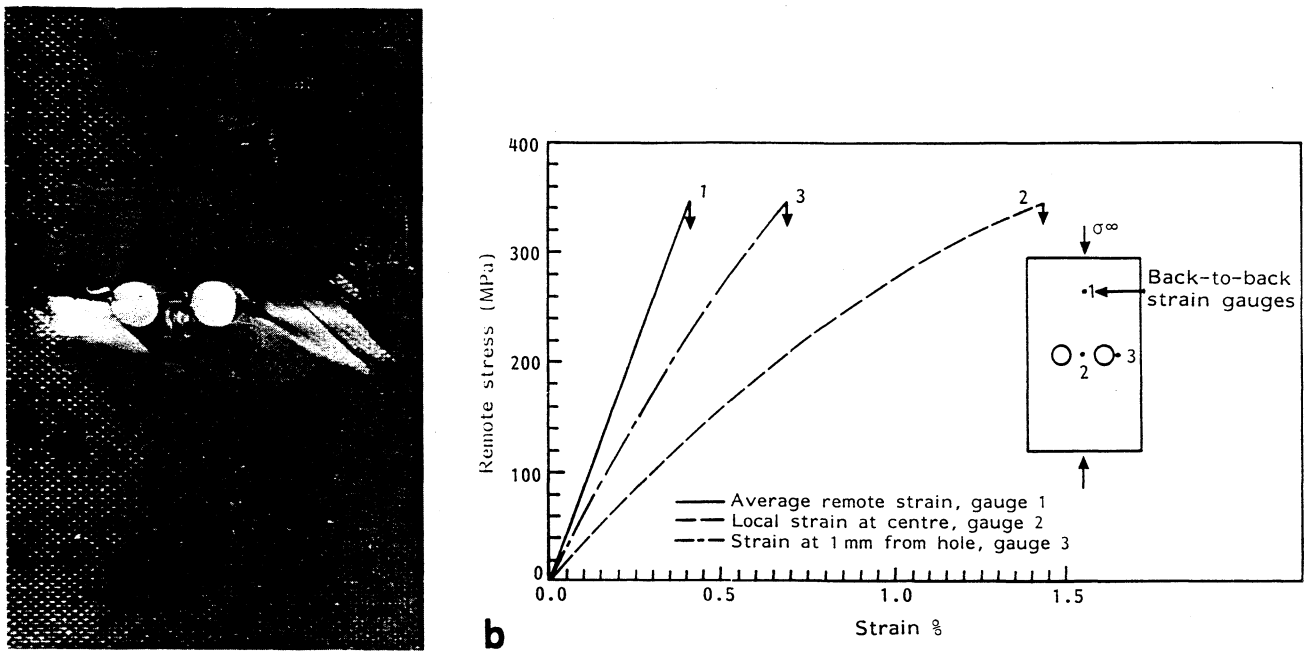

Fig. 6 (a) Overall failure of specimen with two holes at 90° to loading axis. Remote failure strain = 0.4% (a/d = 1.5). (b) Compressive stress/strain response of specimen with two holes perpendicular to loading axis (a/d = 1.5)

mens containing two holes. For $a/d > 2.5$ the stress concentrations for the two geometries are almost identical, and the holes cease to interact as already noted from the measurements of failure load.

Damage mechanisms. A typical penetrant-enhanced X-ray photograph of the damaged induced by static compressive loading in a specimen with a/d = 1.5 geometry is shown in Fig. 8(a). The laminate was loaded at up to 85% of the failure strength and then zinc iodide was applied at the edge of each hole. The X-ray opaque dye penetrates into any crack or delamination and inhances the image of damage. In Fig. 8(a)

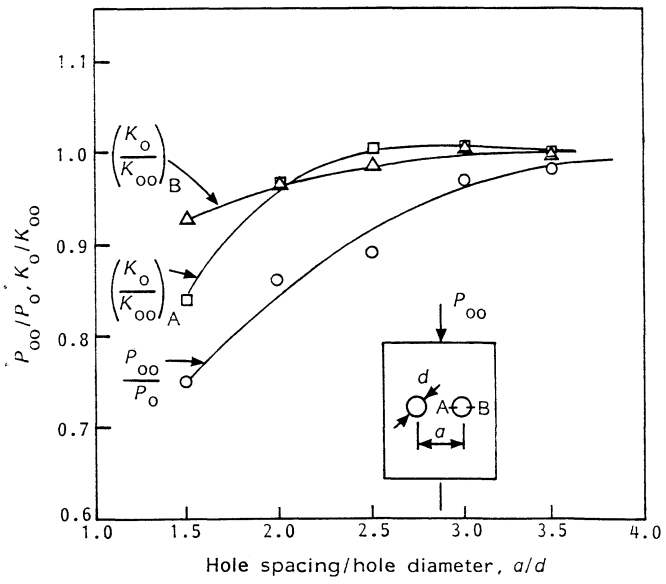

Fig. 7 Hole–hole interaction for two holes of spacing a, diameter d in transverse direction. P_{oo}/P_o is the ratio of failure load for plate with two holes normalized by strength of plate with single hole. K_o/K_{oo} is the ratio of stress concentration factors for single hole and for two holes at locations A and B respectively (see insert)

the region between the holes is heavily cracked and delaminated. Scanning electron microscopy at this load level reveals splitting and microbuckling in the 0° layers; very little damage is observed in the off-axis plies. Fibre microbuckling occurs first in the 0° plies closest to the surface and spreads through the laminate thickness with increasing applied load. In general, it initiates near the location of maximum compressive stress at the hole boundary. However, in Fig. 8(b) the fibre microbuckling in the 0° plies appears to have originated from a point where a 0° split terminates (marked 'A' in Fig. 8(b)). At the tip of the 0° split the stresses are high and cause fibre instability.

On loading the specimen to 95% of the ultimate strength the damage between the holes becomes more severe, see Fig. 8(c). The region between the holes carries little load. The 0° splits have grown and have increased in density. In the 0° central plies the splits tangential to the holes are generally asymmetric. Fig. 8(c), and this is probably related to the centre ply asymmetry, i.e., 0° plies at mid-plane are adjacent to a –45° ply on both sides. Fibre microbuckling of length 1.7 mm and surrounded by delamination extends from the outer edges of the holes. A scanning electron micrograph illustrating fibre microbuckling is shown in Fig. 8(d). Under increasing load the microbuckled region propagates rapidly and the laminate breaks.

From sectioning studies it was observed that two types of fibre microbuckling can occur in the composite laminate: in-plane buckling (X–Y plane) and out-of-plane buckling (Y–Z plane). Some of the outer 0° plies buckle out-of-plane whilst the inner plies fail by predominantly in-plane buckling. In general, out-of-plane microbuckling initiates in areas where the 45°/0° interface is weak (resin-rich regions or high density of voids). Weak ply interfaces reduce fibre support and the fibres buckle outwards at lower compressive loads. Fig. 9 illustrates damage in the 0° central plies of a

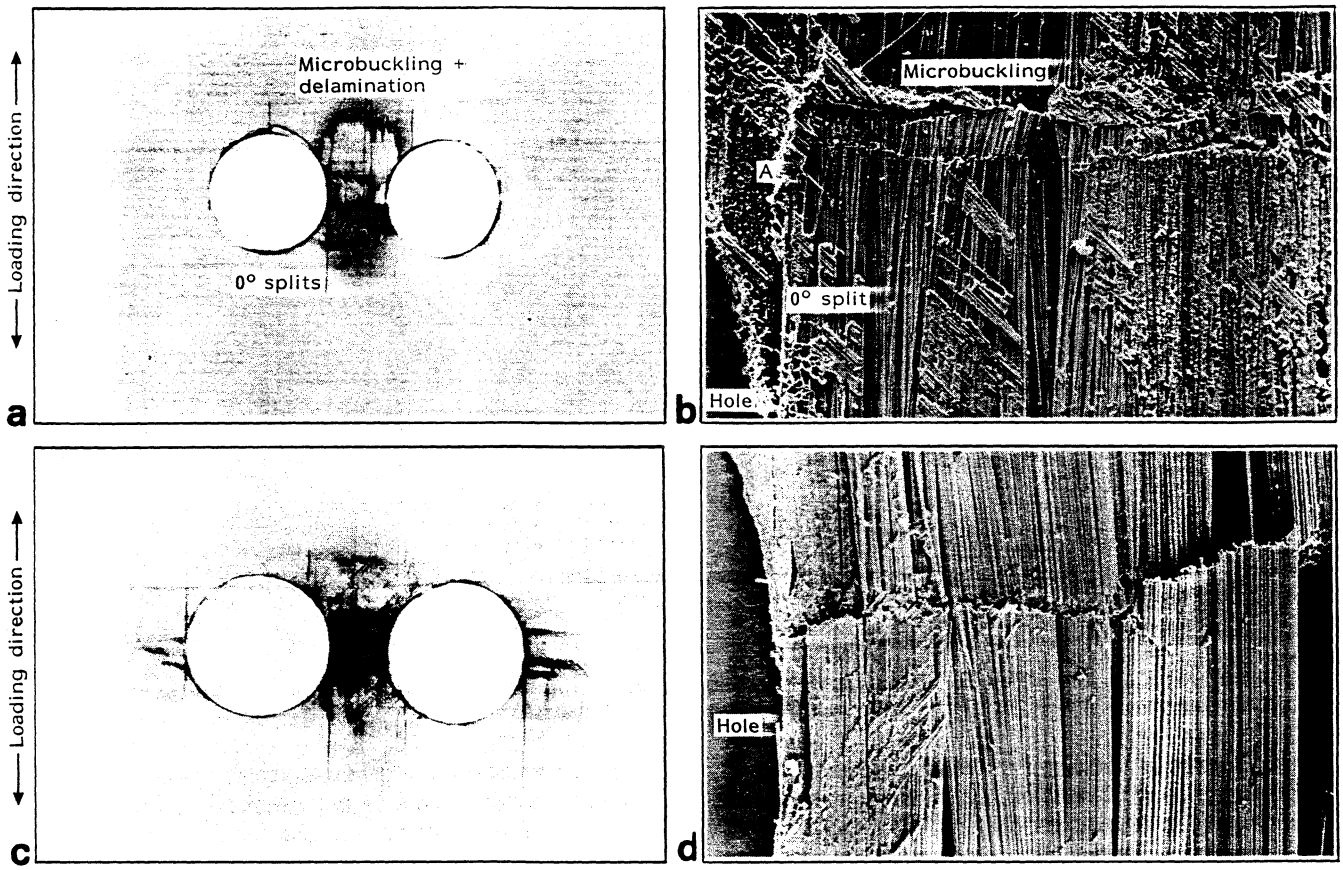

Fig. 8 (a) X-ray radiograph showing damage at about 85% of failure load. Remote strain = 0.35% (a/d = 1.5). (b) Scanning electron micrograph illustrating damage between the two holes in central 0° plies. Remote strain = 0.35% (a/d = 1.5). (c) Damage at 95% of failure load. Remote strain = 0.38% (a/d = 1.5). (d) Fibre microbuckling in a 0° ply growing from the point of maximum compressive stress. Remote strain = 0.38% (a/d = 1.5)

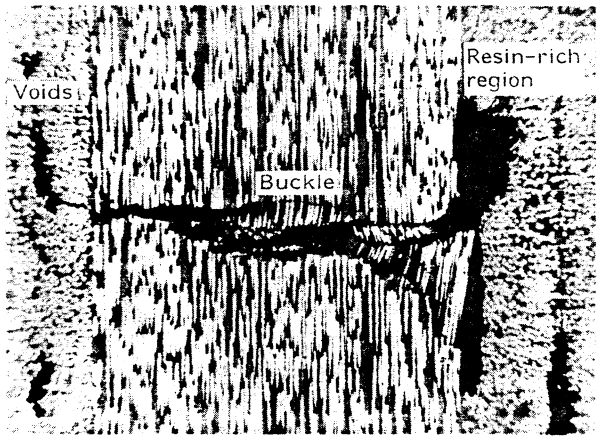

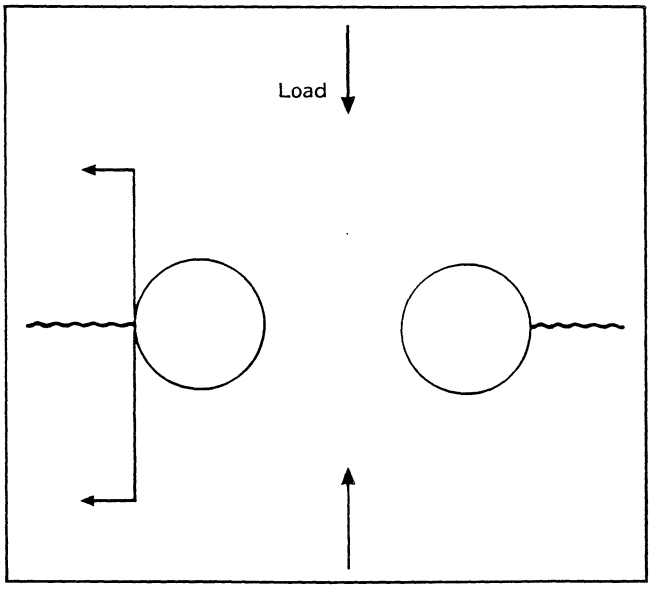

Fig. 9 Out-of-plane microbuckling in the central 0° plies of a notched specimen with high void content and resin-rich areas (a/d = 1.5)

notched specimen with high void content; the 0° fibres buckle out-of-plane at the point where there is insufficient lateral support. The failure strength of specimens with a high concentration of internal defects is 20% lower than that of specimens with fewer defects. Similar observations were made in specimens with a single hole[9].

2. *Specimens with two holes parallel to the loading axis*

Strength data. Fifteen specimens were tested and three hole centre–centre spacings were used. The failure load for the specimens P_{oo} exceeded that for a specimen containing a single hole by up to 20%, see Fig. 10. This

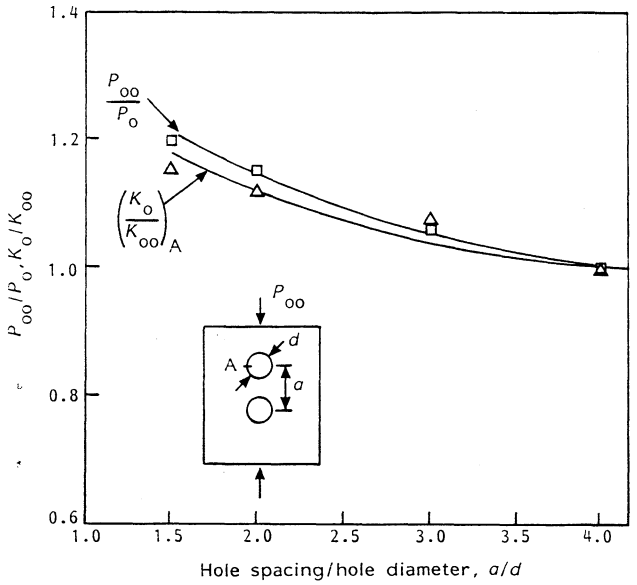

Fig. 10 Hole–hole interaction for two holes of spacing a, diameter d parallel to the loading axis

is consistent with the reduction in stress concentration factor at the edge of the hole when a single hole is replaced by two holes parallel to the loading axis, Fig. 10. Note that for this two hole geometry the net sectional area is equal to that of the specimen containing a single hole. On this basis we define hole–hole interaction to cease when P_{oo}/P_o equals unity. For $a/d \geq 4.0$ the ratio P_{oo}/P_o equals unity and the holes stop to interact. The ratio of stress concentration factors for a single hole and a two hole specimen is in close agreement with the ratio of failure strength for a two hole and a single hole specimen, as shown in Fig. 10.

Damage mechanisms. The failure mechanisms for the composite plate with two holes parallel to the loading direction are similar to those observed in the previous notched cases. At load level equal to 75% of the failure strength a few 0° splits develop at the top and bottom of the hole boundary. Fibre microbuckling initiates at the hole edges in the transverse direction at about 85% of the failure load and it grows with increasing applied load causing failure when it reaches a critical length of 2–3 mm. A typical X-ray radiograph for the $a/d = 2.0$ geometry is shown in Fig. 11; this radiograph was taken after failure. Fibre buckles develop at the edges of both holes, but fracture occurs in the transverse direction through one hole only. For all a/d values investigated ($1.5 \leq a/d \leq 4$), the microbuckling and delamination from one hole did not overlap with that from the other.

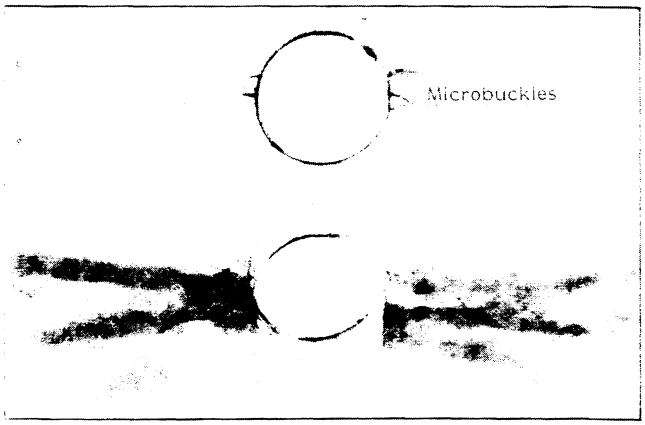

Fig. 11 X-ray radiograph illustrating damage at failure in specimen with two holes parallel to loading axis ($a/d = 2.0$)

3. *Specimens with two holes at 45° to the applied load*

The failure load for specimens containing two holes at 45° to the loading axis is compared with that for the other two hole geometries in Fig. 12. Hole centres aligned at 45° to the loading axis is a particularly weak geometry: for $2.5 \leq a/d \leq 4$ the failure strength is less than that for two holes transverse to the loading axis. For $a/d > 3$ the failure load for the two holes at 45° to the loading axis exceeds 0.9 times the failure load for a specimen containing a single hole. We conclude that hole–hole interaction ceases for $a/d > 3$, since the net sectional area of the two hole specimen resolved transverse to the loading axis equals 0.9 times the net sectional area of the specimen containing a single hole.

Overall failure for the geometry $a/d = 2.0$ is shown in Fig. 13. Failure is by fibre microbuckling on a path between the two holes. For $a/d \geq 2$, the laminate fails through one hole only; the microbuckling and delamination from each hole do not overlap.

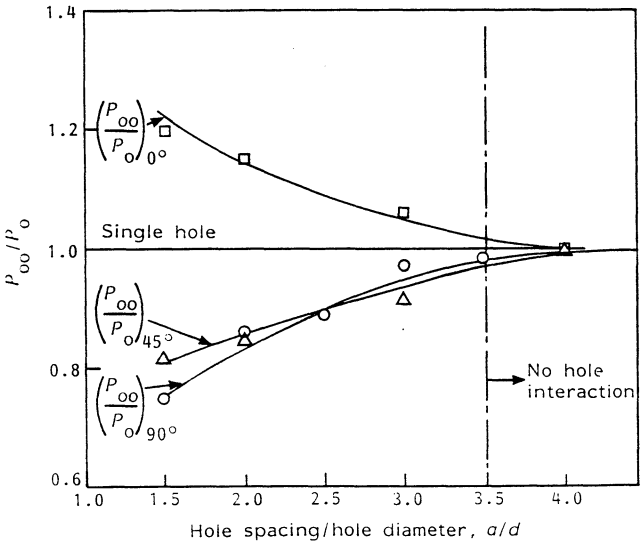

Fig. 12 Failure load of specimen with two holes normalized by the strength of a plate with a single hole

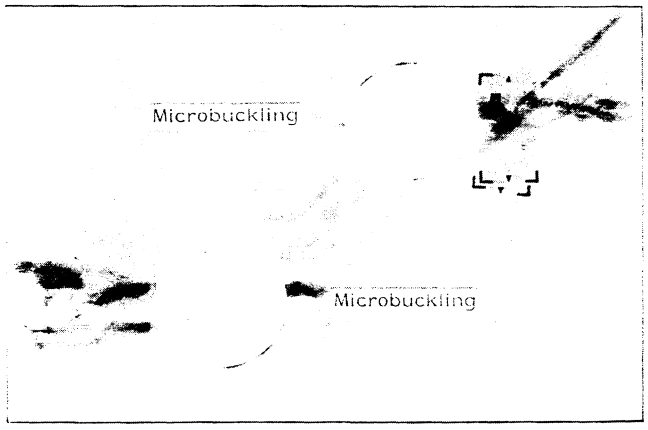

Fig. 13 X-ray radiograph showing damage at failure in a specimen with two holes at 45° to the loading direction ($a/d = 2.0$)

CONCLUDING DISCUSSION

Plain specimens

The unnotched specimens fail by microbuckling of the 0° fibres. The failure strain remote from the microbuckle is the same as for the unidirectional specimens, indicating that the ±45° plies have no significant influence on the failure strength of the axial plies.

Single hole specimens

The effect of a single 5 mm diameter hole in a 50 mm wide plate is to reduce the failure load by 47%. The critical failure mechanism is fibre microbuckling in the 0° plies surrounded by delamination. It initiates at the edges of the hole at 85% of the fracture stress and occurs first in the outer 0° plies. The local strain at microbuckling initiation is 1.5%, which is 25% higher than the failure strain of the unnotched specimens. The higher strain for triggering from the edge of a single hole is due to the constraint of undamaged elastic material surrounding the microbuckled zone. With increased applied load the buckle zone grows across the specimen width. The extent of the buckled zone prior to catastrophic failure is 2–3 mm.

Two hole specimens

Specimens were tested with two holes placed transverse to the loading axis, parallel and at 45° to the loading axis. For the three geometries, hole–hole interaction has ceased and the failure load equals that for a specimen containing a single hole when the hole–hole centre spacing exceeds four times the hole diameter. Failure is by microbuckling of the 0° fibres for all orientations of the two holes. Microbuckling initiates at 80–85% of the failure load and grows stably from the outer edge of each hole for 2–3 mm before catastrophic failure occurs. The effect of hole–hole spacing upon compressive strength is similar qualitatively to the effect upon the stress concentration factor at the edge of each hole. For holes transverse and at 45° to the loading axis a decrease in hole–hole spacing gives rise to an increase in stress concentration factor and a decrease in compressive strength. For holes aligned with the loading axis, a decrease in hole–hole spacing causes the stress concentration factor to decrease and the compressive strength to increase.

ACKNOWLEDGEMENTS

The authors are grateful for funding from the Procurement Executive of the Ministry of Defence, under a joint SERC/MOD contract.

REFERENCES

1 **Ewins, P.D. and Potter, R.T.** 'Some observations on the nature of fibre reinforced plastics and the implications for structural design' *Phil Trans R Soc Lond* **A294** (1980) pp 507–517
2 **Port, K.F.** 'The compressive strength of CFRP' *RAE Technical Report TR-82083* (1982)
3 **Potter, R.T.** 'The environmental degradation of notched CFRP in compression' *Composites* **14** No 3 (1983) pp 206–225
4 **Rhodes, M.D., Mikulas, M.M. and McGowan, P.E.** 'Effects of orthotropy and width on the compression strength of graphite–epoxy panels with holes' *AIAA Journal* **22** No 9 (1984) pp 1283–1292
5 **Curtis, P.T. and Dorey, G.** 'Hole interactions in CFRP and aluminium alloys' *RAE Technical Report TR-79138* (1979)
6 **Snell, M.B.** 'Strength and elastic response of symmetric angle-ply CFRP' *RAE Technical Report TR-76091* (1976)
7 **Curtis, P.T.** 'CRAG test methods for the measurement of the engineering properties of fibre reinforced plastics' *RAE Technical Report TR-85099* (1985)
8 **Soutis, C., Smith, P.A. and Fleck, N.A.** 'Investigation of notched compressive strength of CFRP' *2nd Int Symp on Phase Interaction in Composite Materials, Patras, Greece, August 1988*
9 **Soutis, C. and Fleck, N.A.** 'Static compression failure in carbon fibre–epoxy T800/924C composite plate with a single hole' *J Comp Mater* **24** No 5 (May 1990) pp 536–558
10 **Scott, I.G. and Scala, C.M.** 'A review of non-destructive testing of composite materials' *NDT International* **12** (1982) p 75
11 **Freeman, S.M.** 'Characterization of lamina and interlaminar damage in graphite/epoxy composites by deply technique' *Composite Materials: Testing and Design (6th Conference), ASTM STP 787* (1982) pp 50–62
12 **Green, A.E.** *Proc Roy Soc London* **180A** (1942) p 173

AUTHORS

C. Soutis and N.A. Fleck are with Cambridge University Engineering Department, Trumpington Street, Cambridge CB2 1PZ, UK. P.T. Curtis is with the Materials and Structures Department, Royal Aerospace Establishment, Farnborough GU14 6TD, UK.